Mechanisms Underlying Proton Release in CLC-type F^-/H^+ Antiporters

Maria Gabriella Chiariello,[†, #, §, *] Mercedes Alfonso-Prieto,[†,⊥] Emiliano Ippoliti,[†, §] Christoph Fahlke,[#,‡,*] Paolo Carloni[†,§,¶,‡^,*]

† Institute for Advanced Simulation (IAS-5) and Institute of Neuroscience and Medicine (INM-9), Computational Biomedicine, Forschungszentrum Jülich, 52425 Jülich, Germany

Institute of Biological Information Processing (IBI-1), Molekular- und Zellphysiologie, Forschungszentrum Jülich, 52425 Jülich, Germany

§ JARA-HPC, Forschungszentrum Jülich, 54245 Jülich, Germany

⊥ Cécile and Oskar Vogt Institute for Brain Research, University Hospital Düsseldorf, Medical Faculty, Heinrich Heine University Düsseldorf, 40225 Düsseldorf, Germany

¶ Department of Physics, RWTH Aachen University, 52056 Aachen, Germany

^ JARA Institute Molecular neuroscience and neuroimaging (INM-11), Forschungszentrum Jülich, 52425 Jülich, Germany

* Corresponding authors

Supporting Information Placeholder

ABSTRACT: The CLC family of anion channels and transporters includes Cl^-/H^+ exchangers (blocked by F^-) and F^-/H^+ exchangers (or CLC^Fs). CLC^Fs contain a glutamate (E318) in the central anion-binding site, that is absent in CLC Cl^-/H^+ exchangers. The X-ray structure of the protein from *Enterococcus casseliflavus* (CLC^F-eca) shows that E318 tightly binds to F^- when the gating glutamate (E118; highly conserved in the CLC family) faces the extracellular medium. Here we use classical and DFT-based QM/MM metadynamics simulations to investigate proton transfer and release by CLC^F-eca. After *up* to *down* movement of protonated E118, both glutamates combine with F^- to form a triad, from which protons and F^- anions are released as HF. Our results illustrate how glutamate insertion into the central anion-binding site of CLC^F-eca permits the release of H^+ to the cytosol as HF, thus enabling a net 1:1 F^-/H^+ stoichiometry.

Keywords: ion channels, QM/MM, free energy, metadynamics

Fluoride can permeate cell membranes as HF [1], in contrast to other anions such as Cl^- and NO_3^-. HF is a weak acid (pKa ~ 3.2 [2]) that does not dissociate completely in water. Inside the cytoplasm, F^- anions may inhibit enzymes necessary for energy production and nucleic acid synthesis at concentrations close to environmental levels [3,4]. This occurs because of the peculiar chemical properties of F^-: the anion is isosteric with hydroxide[5] and can form strong coordination complexes with Mg^{2+} and phosphate[6], thus acting as transition state-like inhibitor of several enzymatic reactions. The strong selectivity of most anion channels and transporters against F^- limits its resorption in the gastrointestinal tract of higher organisms. Unicellular organisms accumulate F^- intracellularly, but specialized F^- transporters in bacteria, protozoa or yeast reduce intracellular fluoride to below toxic concentrations. One such group of F^- transporters, the CLC^F transporters [7-8], belongs to the large CLC family of anion channels and transporters [9-11]. CLC^F transporters exchange H^+ and F^- with 1:1 stoichiometry [7, 12], thus exploiting the proton influx in acidic environments to clear F^- from the bacterial cytoplasm. CLC^F transporters are closely related to the prototypic CLC-type Cl^-/H^+ exchanger from *Escherichia coli*, CLC-ec1 [12]. However, whereas CLC-ec1 is a chloride transporter that is strongly inhibited by F^- [13], CLC^Fs are effective F^- transporters.

Functional and structural analyses [7, 12, 14] have demonstrated shared mechanisms for CLC^F basic transport and CLC-ec1 Cl^-/H^+ exchange; the latter has been studied in great detail in recent years [15-26]. In CLC-ec1, Cl^-/H^+ exchange critically depends on two conserved glutamate residues: the gating glutamate (E148) [27] and the internal glutamate (E203) [17, 19]. During transport, E148 moves up and down [28-31], shuttling protons from one membrane site to the other, whereas E203 is

necessary for proton release into the internal medium [17, 19]. Proton movement drives Cl^- transport in the opposite direction, resulting in a Cl^-/H^+ exchange at 2:1 stoichiometry [32]. F^- blocks CLC-ec1 by forming a strong hydrogen bond (H-bond) with the gating E148 [13]. This H-bond locks the glutamate in a conformation that does not allow proton transport. In contrast, CLC^F proteins exchange fluoride and protons with 1:1 stoichiometry [7, 12, 14]. Thus, they differ from CLC-ec1 in both halide selectivity and transport stoichiometry. The *Enterococcus casseliflavus* CLC^F exchanger (CLC^F-eca) lacks the intracellular transport glutamate [12], but contains a glutamate close to the central anion-binding site (E318, Figures 1 and S1).

Here, we use classical and quantum mechanics/molecular mechanics (QM/MM) combined with well-tempered metadynamics (WT-MTD) [33-34] simulations to study how CLC^F transporters discriminate F^- from Cl^-. We employed the highly parallel interface (MiMiC)[35] between the CPMD and GROMACS codes for the QM (B3LYP and BLYP-based DFT) [36-37] and MM (CHARMM) [38] calculations, respectively.

Our simulations focus on the first transport steps that result in H^+ movement from outside to inside the cell, using the X-ray structure of wild-type CLC^F-eca [12] as the starting conformation. Here, the gating glutamate (E118) is in the *up* conformation and is free to exchange protons with the extracellular solution. E318 is located in the central anion-binding site S_{cen}. Its close contact with fluoride in the CLC^F-eca X-ray structure[12] (F^-_{cen} in Figures 1 and S2A) suggests that E318 must be protonated in this conformation. Thus, we assume that both E118 and E318 are protonated. Further details on the choice of protonation state of the two glutamates are given in the Supporting Information (page S2).

After 300 ns of classical MD simulation (Figure S3), we studied the conformational change of E118 via classical WT-MTD. The calculated free energy profile as a function of the E118 N-Cα-Cβ-Cγ (χ_1) dihedral angle (Figure 2A) shows that the *up* to *down* transition of protonated E118 is barrierless. The global minimum corresponds to E118 in the *down* conformation (Figure 2A), with both glutamate protons interacting with F^-_{cen} to form an E318-F-E118 triad.

To investigate the location of the protons in each of the two E118 conformations, we next computed proton transfer free energies by QM/MM WT-MTD. In the E118 *up* conformation, F^-_{cen} interacts only with the coordinating glutamate E318, forming a strong H-bond. By calculating the free energy as a function of the H(E318)-F^- distance (Figures 2B and S4), we found a single minimum at a distance of 1.5 Å[39].

When E118 adopts the *down* position, F^- becomes coordinated by both glutamates. The free energy surface as a function of the H(E118)-F^- and H(E318)-F^- distances (Figures 2C and S6) shows a single minimum corresponding to an HF molecule located between protonated E118 and deprotonated E318 (i.e. H(E118)-F= 1.7 Å and H(E318)-F = 1.1 Å). An overlap of the QM/MM free energy profiles for the two E118 positions (Figure 2B; *up* vs *down*) projected onto the H(E318)-F distance illustrates a free energy minimum shift from 1.5 Å to 1.1 Å during the *up* to *down* movement of E118. Such shortening of the H(E318)-F distance indicates a change from F^- that is H-bonded to protonated E318 (*up* position) to HF that is H-bonded to deprotonated E318 (*down* position).

To understand the release of the resulting HF to the intracellular solution, we next calculated the QM/MM WT-MTD free energy surface (Figure 3A) as function of the H(E118)-F and H(E118)-O(E318) distances (Figure S8 gives a graphical definition). These two collective variables describe the release of HF from the gating glutamate and the approach of the two glutamates, respectively. Three free energy minima are identified (Figure 3A). These differ by only 2 kcal/mol or less and are separated by low barriers (around 5 kcal/mol), indicating that their interconversion is possible at 300 K. One minimum **(i)** corresponds to the E318-F-E118 triad from the previous simulation, in which the H(E118)-F and H(E118)-O(E318) distances are 1.5 Å and 3.3 Å, respectively. In **(ii)**, the gating E118 is dissociated from both HF (H(E118)-F = 3.5 Å) and E318 (H(E118)-O(E318) = 3.5 Å). In **(iii)**, HF is no longer H-bonded to E118 (H(E118)-F = 3 Å), but instead forms an H-bond with the E318 carboxyl group (Figure 3A, inset). Here, E118 is protonated and H-bonded with E318 (H(E118)-O(E318) = 1.5 Å). Thus, our simulations suggest that after inward proton release as HF, E118 and E318 form an H-bonded dyad. We noted that the distance between the two glutamates within the dyad is similar to that observed in the V319G CLC^F-eca X-ray structure [12] (see Figure S2B).

We next investigated the energetics associated with HF release from E318. A QM/MM WT-MTD calculation provides the free energy as a function of the distance between the HF hydrogen and the O1 of E318 (for oxygen atom labels, see Figure 3B insets and Figure S9). The first two minima are isoenergetic and separated by a barrier lower than 2 kcal/mol, indicating that HF can be H-bonded to either oxygen atom of the E318 carboxyl group. For HF dissociation from the coordinating glutamate (O1(E318)-HF = 6 Å) a barrier of about 4 kcal/mol needs to be overcome. This results in HF being solvated by water molecules in the intracellular side of the channel, while E318 remains in contact with the gating glutamate (E118) in the *down* conformation. This

simulation was performed with a harmonic restraint on the HF distance to facilitate convergence of the free energy surface (see the Supporting Information for details). Since our model does not include the possibility of HF dissociation, the free energy profile in Figure 3B can be considered a lower bound limit of the energy for HF release from the glutamates to the intracellular solution. Nonetheless, HF in the intracellular vestibule of CLC^F-eca is solvated exclusively by water molecules; the absence of strong H-bond donors disfavours HF dissociation with long-range proton diffusion[40-41].

In summary, our calculations suggest that protonation of E118 leads to a barrierless transition from the *up* to *down* conformation to form a E318-F-E118 triad stabilized by a complex H-bond network (Figure 4). This triad allows protonation of fluoride to form HF, which becomes H-bonded to both protonated E118 and deprotonated E318. Next, E118 approaches E318, expelling HF from the central binding site and resulting in formation of the E318-E118 dyad. HF swings between the two carboxyl oxygen atoms of E318 and is then released into the intracellular solution, leaving the two glutamates in contact and occupying the central binding site of CLC^F-eca. In CLC-ec1, only a single glutamate/fluoride interaction is possible with the gating E148, which causes fluoride blockage via proton sharing between the glutamate and fluoride [13]. Instead, CLC^F-eca prevents fluoride blockage by forming the E118-F-E318 triad that permits release of HF from the central binding site.

The simultaneous release of protons and fluoride ions into the internal solution was proposed to explain the reduced stoichiometry of H^+/F^- exchange compared with Cl^-/H^+ exchange[7, 12]. Our calculations put forward the detailed molecular mechanism of this co-release (Figure S10). Downward rotation of the protonated E118, together with projection of the CLC^F-eca-specific E318 toward the central binding site, enables fluoride protonation and subsequent release as HF into the intracellular solution.

CLC^Fs select against Cl^-, the main physiological halide, via weaker binding and a strongly voltage-dependent chloride translocation that greatly enhances F^- selectivity at physiological voltages[14]. F^- forms either partially or fully covalent bonds with the protons in the E118-F-E318 system (Figure 4). In contrast, Cl^- can only form ionic H-bonds with the two glutamates [42]. Moreover, Cl^- is an extremely weak base (pKa = -7) that cannot accept a proton from E318 (pKa = 4.2).

Combined mutagenesis and functional studies have demonstrated that neutralizing the gating glutamate (E118Q and E118A) abolishes proton and F^- transport, resulting in Cl^- fluxes that are inhibited by F^-[12]. In the E118 mutants, anion transport is not linked to the counter transport of H^+ as in the WT[12]. These mutants possess only one glutamate (E318), and the presence of a single fluoride-glutamate interaction can account for the observed F^- blockage[12], as in the case of CLC-ec1 [13, 42]. A similar argument was recently put forward using electrostatic calculations[43]. One might speculate that E118 (in the *middle* position shown in Figure S10) electrostatically weakens the E318-F interaction in WT CLC^F-eca, whereas neutralization of E118 (E118Q or E118A) prevents effective release of F^- from E318.

In contrast, mutations of the coordinating E318 still permit coupled H^+/F^- transport. However, the E318A and E318Q mutations changed the transport stoichiometry from 1:1 to 2:1 [12]. Our simulations suggest that HF formation and release is hampered in these mutants because of the removal of the second glutamate in the central binding site. Nonetheless, these mutants may release H^+ from the gating E118, thus permitting F^--H^+ exchange. The ability of E118 to release H^+ is supported by the proton-coupled Cl^- transport observed in WT CLC^F-eca [14].

The E318 mutations strongly reduce F^- transport rates [12]. At present, our simulations cannot provide a rationale for this reduction. We also do not understand the difference between the E318A/Q CLC^F-eca mutants and CLC-ec1, which both lack glutamate at the E318 position but differ in F^- inhibition. It is possible that replacement of S107 (which coordinates the anion at S_{cen} in CLC-ec1) by M79 in CLC^F-eca prevents fluoride block in E318A/Q CLC^F-eca mutants. This is supported by the differences in anion selectivity between the two CLC^F subclades [14]. Members of the MV subclade (such as CLC^F-eca, with M79 and V82 in the central anion-binding site) exhibit a higher selectivity for fluoride over chloride, compared to members of the NT subclade.

The V319G mutation has a threefold reduction in transport rates, yet with 2:1 F^-/H^+ stoichiometry. The corresponding X-ray structure shows a change in the orientation of E318 [12]. Based on our simulations, we further suggest that this mutant might impair triad formation and thus hinder HF formation.

Our simulations provide insight into F^- binding at the CLC^F-eca central anion site and H^+ release as HF to the internal medium. They also lead to a prediction to be tested in future studies: If two glutamate residues are crucial for fluoride transport at 1:1 F^-/H^+ stoichiometry, then insertion of a second glutamate into the coordination sphere of the chloride in a CLC-type Cl^-/H^+ exchanger should be the first step to convert the chloride transporter into a fluoride transporter (although further substitutions might be needed to shift chloride transport towards highly negative, non-physiological voltages). F^- transport by CLC^F-eca demonstrates how evolution overcomes the chemical features of substrates to generate selective transporters.

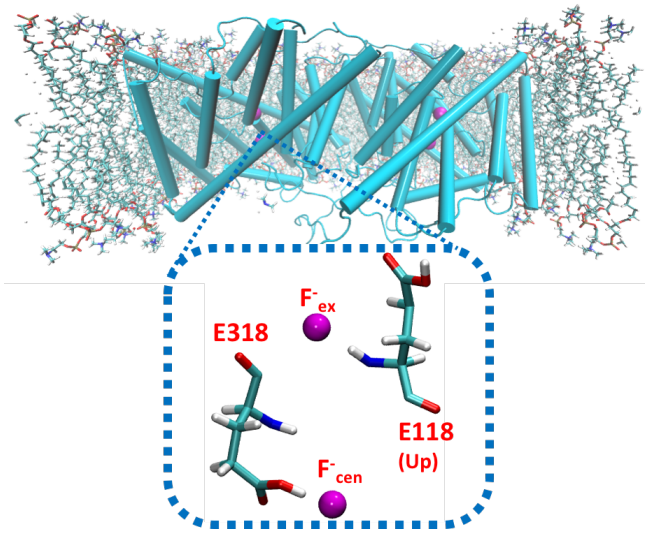

FIGURE 1. Top panel: *E. casseliflavus* F^-/H^+ antiporter (CLC^F-eca) embedded in a lipid bilayer in our simulation setup. Water and counterions are not shown for clarity. **Bottom panel:** Anion-binding sites in the wild-type protein. The two fluoride anions (F^-_{ex} and F^-_{cen}) present in the crystal structure (PDB code 6D0J) are included in our simulations. F^-_{cen} is coordinated by E318 and the gating glutamate E118 is in the *up* conformation.

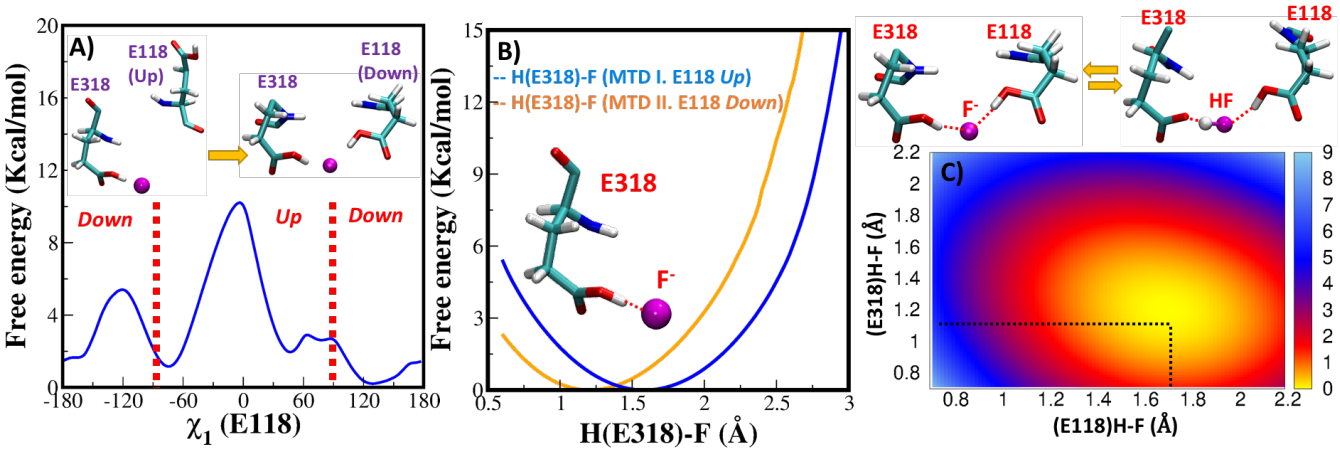

FIGURE 2. A) Classical MTD simulation of conformational change in the gating glutamate. *Up*/*down* conformations are defined by the position of the E118 side chain above/below the plane of the backbone. Red dashed lines indicate the transition between conformations. **B) QM/MM MTD of proton transfer between fluoride and E318** with the gating glutamate E118 in either the *up* (MTD.I, blue) or *down* (MTD.II, orange) conformation. **C) QM/MM MTD.II of double proton transfer in the E118-F-E318 triad with the gating glutamate E118 in the *down* conformation**. The two possible H-bond networks are shown on the right, with H-bonds indicated as red dashed lines. The free energy profiles are in kcal/mol.

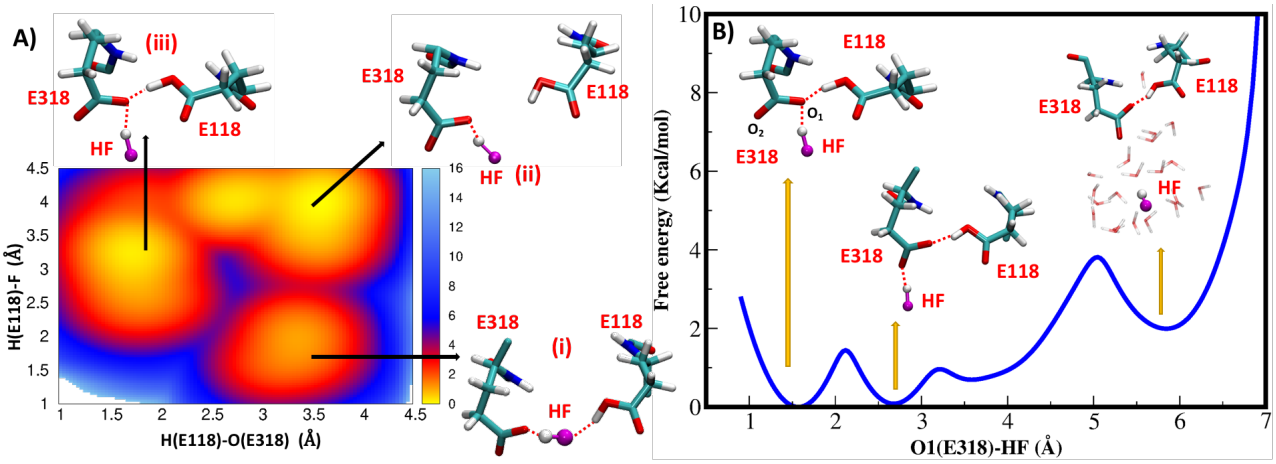

FIGURE 3. A) QM/MM MTD.III of conversion of the E318-F-E118 triad into the intermediate conformation with E318 and E118 in direct contact. B) QM/MM MTD.IV of HF release into the intracellular solution. The E318 carboxyl oxygen atoms are labelled O1 and O2. H-bonds are shown as red dashed lines and free energy profiles are in kcal/mol.

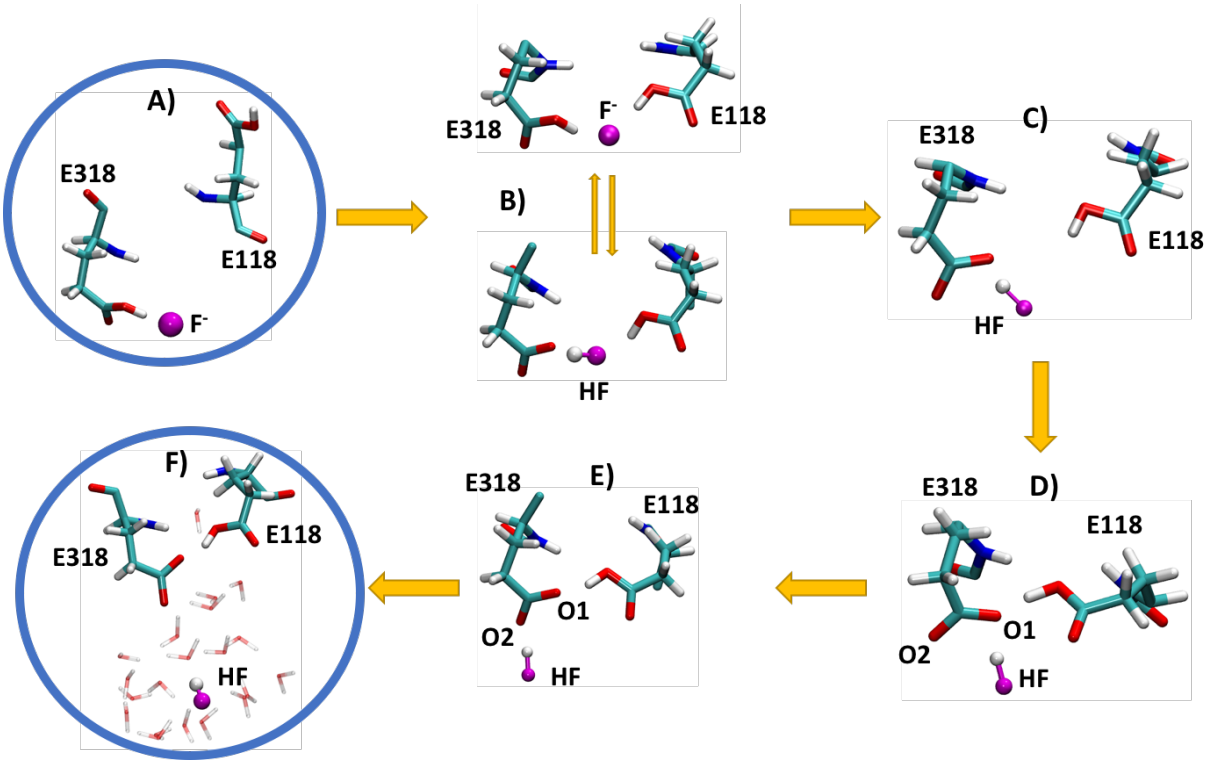

FIGURE 4. Structures involved in the conversion of conformation A (corresponding to the wild-type CLC^F-eca crystal structure) to intermediate F (proposed based on the V319G X-ray structure[12]). A) E118 is in the *up* conformation and exposed to the extracellular solution, where it can easily exchange protons. **B)** Protonated E118 undergoes a spontaneous *up* to *down* transition, leading to formation of the E318-F-E118 triad. In the *down* conformation, E118 interacts directly via an H-bond with $F^-_{cen.}$, which accepts a proton from E318 to form HF. **C)** Gating E118 dissociates from the anion and approaches the carboxyl oxygen of E318. **D)** E318 and E118 are in close proximity and interact via an H-bond. HF is still H-bonded to one of the E318 carboxyl oxygen atoms. **E)** HF swings between the two E318 carboxyl oxygen atoms and finally dissociates into the intracellular solution. **F)** E118 in the *down* conformation has replaced fluoride in the central binding site; HF is surrounded by water molecules in the intracellular part of the vestibule.

ASSOCIATED CONTENT

Supporting Information

The Supporting Information is available free of charge on the ACS Publications website.

It includes computational details for the system setup, classical MD, and classical and QM/MM MTD simulations; structural analysis of the MD simulation; and convergence of the free energy profiles for all QM/MM MTD simulations presented in this work (MTD.I-IV).

AUTHOR INFORMATION

Corresponding Author

g.chiariello@fz-juelich.de

c.fahlke@fz-juelich.de

p.carloni@fz-juelich.de

Author Contributions

‡These authors contributed equally.

Notes

The authors declare no competing financial interest.

ACKNOWLEDGMENT

M.A.P., C.F., and P.C. are funded by Deutsche Forschungsgemeinschaft via the Research Unit FOR2518 “Functional Dynamics of Ion Channels and Transporters – DynIon”, project P6. The authors gratefully acknowledge the Gauss Centre for Supercomputing e.V. (GSC; www.gauss-centre.eu) for providing computing time on the GCS Supercomputer JUWELS[44] at the Jülich Supercomputing Centre.

REFERENCES

1. Orabi, E. A.; Faraldo-Gómez, J. D., New Molecular-Mechanics Model for Simulations of Hydrogen Fluoride in Chemistry and Biology. *J. Chem. Theory Comput.* **2020,** *16* (8), 5105-5126.
2. Cotton, F. A.; Wilkinson, G.; Murillo, C. A.; Bochmann, M.; Grimes, R., *Advanced Inorganic Chemistry*. Wiley New York: 1988.
3. Zuo, H.; Chen, L.; Kong, M.; Qiu, L.; Lü, P.; Wu, P.; Yang, Y.; Chen, K., Toxic Effects of Fluoride on Organisms. *Life Sci.* **2018,** *198*, 18-24.
4. Adamek, E.; Pawlowska-Goral, K.; Bober, K., In Vitro and in Vivo Effects of Fluoride Ions on Enzyme Acivity *Ann. Acad. Med. Stetin.* **2005,** *51* (2), 69.
5. Qin, J.; Chai, G.; Brewer, J. M.; Lovelace, L. L.; Lebioda, L., Fluoride Inhibition of Enolase: Crystal Structure and Thermodynamics. *Biochemistry* **2006,** *45* (3), 793-800.
6. Goličnik, M.; Olguin, L. F.; Feng, G.; Baxter, N. J.; Waltho, J. P.; Williams, N. H.; Hollfelder, F., Kinetic Analysis of β-Phosphoglucomutase and Its Inhibition by Magnesium Fluoride. *J. Am. Chem. Soc.* **2009,** *131* (4), 1575-1588.
7. Stockbridge, R. B.; Lim, H.-H.; Otten, R.; Williams, C.; Shane, T.; Weinberg, Z.; Miller, C., Fluoride Resistance and Transport by Riboswitch-Controlled CLC Antiporters. *Proc. Natl. Acad. Sci.* **2012,** *109* (38), 15289.
8. McIlwain, B. C.; Ruprecht, M. T.; Stockbridge, R. B., Membrane Exporters of Fluoride Ion. *Ann. Rev. Biochem.* **2021,** *90* DOI: 10.1146/annurev-biochem-071520-112507.
9. Jentsch, T. J.; Stein, V.; Weinreich, F.; Zdebik, A. A., Molecular Structure and Physiological Function of Chloride Channels. *Physiol. Rev.* **2002,** *82* (2), 503-568.
10. Stölting, G.; Fischer, M.; Fahlke, C., CLC Channel Function and Dysfunction in Health and Disease. *Front. Physiol.* **2014,** *5*, 378.
11. Poroca, D. R.; Pelis, R. M.; Chappe, V. M., ClC Channels and Transporters: Structure, Physiological Functions, and Implications in Human Chloride Channelopathies. *Front. Pharmacol.* **2017,** *8*, 151.
12. Last, N. B.; Stockbridge, R. B.; Wilson, A. E.; Shane, T.; Kolmakova-Partensky, L.; Koide, A.; Koide, S.; Miller, C., A CLC-type F-/H+ Antiporter in Ion-Swapped Conformations. *Nat. Struct. Mol. Biol.* **2018,** *25* (7), 601-606.
13. Chiariello, M. G.; Bolnykh, V.; Ippoliti, E.; Meloni, S.; Olsen, J. M. H.; Beck, T.; Rothlisberger, U.; Fahlke, C.; Carloni, P., Molecular Basis of CLC Antiporter Inhibition by Fluoride. *J. Am. Chem. Soc.* **2020,** *142* (16), 7254-7258.
14. Brammer, A. E.; Stockbridge, R. B.; Miller, C., F−/Cl− Selectivity in CLCF-type F−/H+ Antiporters. *J. Gen. Physiol.* **2014,** *144* (2), 129-136.
15. Dutzler, R.; Campbell, E. B.; Cadene, M.; Chait, B. T.; MacKinnon, R., X-ray Structure of a ClC Chloride Channel at 3.0 Å Reveals the Molecular Basis of Anion Selectivity. *Nature* **2002,** *415* (6869), 287-294.
16. Accardi, A.; Miller, C., Secondary Active Transport Mediated by a Prokaryotic Homologue of ClC Cl- Channels. *Nature* **2004,** *427* (6977), 803-807.
17. Accardi, A.; Walden, M.; Nguitragool, W.; Jayaram, H.; Williams, C.; Miller, C., Separate Ion Pathways in a Cl-/H+ Exchanger. *J. Gen. Physiol.* **2005,** *126* (6), 563.
18. Jiang, T.; Han, W.; Maduke, M.; Tajkhorshid, E., Molecular Basis for Differential Anion Binding and Proton Coupling in the Cl–/H+ Exchanger ClC-ec1. *J. Am. Chem. Soc.* **2016,** *138* (9), 3066-3075.
19. Chavan, T. S.; Cheng, R. C.; Jiang, T.; Mathews, I. I.; Stein, R. A.; Koehl, A.; McHaourab, H. S.; Tajkhorshid, E.; Maduke, M., A CLC-ec1 Mutant Reveals Global Conformational Change and Suggests a Unifying Mechanism for the CLC Cl–/H+ Transport Cycle. *eLife* **2020,** *9*, e53479.
20. Dutzler, R.; Wang, Y. F.; Rizkallah, P. J.; Rosenbusch, J. P.; Schirmer, T., Crystal Structures of Various Maltooligosaccharides Bound to Maltoporin Reveal a Specific Sugar Translocation Pathway. *Structure* **1996,** *4* (2), 127-134.
21. Walden, M.; Accardi, A.; Wu, F.; Xu, C.; Williams, C.; Miller, C., Uncoupling and Turnover in a Cl−/H+ Exchange Transporter. *J. Gen. Physiol.* **2007,** *129* (4), 317-329.
22. Picollo, A.; Malvezzi, M.; Houtman, J. C. D.; Accardi, A., Basis of Substrate Binding and Conservation of Selectivity in the CLC Family of Channels and Transporters. *Nat. Struct. Mol. Biol.* **2009,** *16* (12), 1294-1301.
23. Basilio, D.; Noack, K.; Picollo, A.; Accardi, A., Conformational Changes Required for H+/Cl− Exchange Mediated by a CLC Transporter. *Nat. Struct. Mol. Biol.* **2014,** *21* (5), 456-463.
24. Han, W.; Cheng, R. C.; Maduke, M. C.; Tajkhorshid, E., Water Access Points and Hydration Pathways in CLC H+/Cl- Transporters. *Proc. Natl. Acad. Sci.* **2014,** *111* (5), 1819.
25. Khantwal, C. M.; Abraham, S. J.; Han, W.; Jiang, T.; Chavan, T. S.; Cheng, R. C.; Elvington, S. M.; Liu, C. W.; Mathews, I. I.; Stein, R. A.; McHaourab, H. S.; Tajkhorshid, E.; Maduke, M., Revealing an Outward-Facing Open Conformational State in a CLC Cl–/H+ Exchange Transporter. *eLife* **2016,** *5*, e11189.
26. Lobet, S.; Dutzler, R., Ion-Binding Properties of the ClC Chloride Selectivity Filter. *EMBO J.* **2006,** *25* (1), 24-33.
27. Dutzler, R.; Campbell, E. B.; MacKinnon, R., Gating the Selectivity Filter in ClC Chloride Channels. *Science* **2003,** *300* (5616), 108.
28. Mayes, H. B.; Lee, S.; White, A. D.; Voth, G. A.; Swanson, J. M. J., Multiscale Kinetic Modeling Reveals an Ensemble of Cl–/H+ Exchange Pathways in ClC-ec1 Antiporter. *J. Am. Chem. Soc.* **2018,** *140* (5), 1793-1804.
29. Lee, S.; Mayes, H. B.; Swanson, J. M. J.; Voth, G. A., The Origin of Coupled Chloride and Proton Transport in a Cl–/H+ Antiporter. *J. Am. Chem. Soc.* **2016,** *138* (45), 14923-14930.
30. Lee, S.; Swanson, Jessica M. J.; Voth, Gregory A., Multiscale Simulations Reveal Key Aspects of the Proton Transport Mechanism in the ClC-ec1 Antiporter. *Biophys. J.* **2016,** *110* (6), 1334-1345.
31. Vien, M.; Basilio, D.; Leisle, L.; Accardi, A., Probing the Conformation of a Conserved Glutamic Acid Within the Cl− Pathway of a CLC H+/Cl− Exchanger. *J. Gen. Physiol.* **2017,** *149* (4), 523-529.
32. Picollo, A.; Xu, Y.; Johner, N.; Bernèche, S.; Accardi, A., Synergistic Substrate Binding Determines the Stoichiometry of Transport of a Prokaryotic H+/Cl− Exchanger. *Nat. Struct. Mol. Biol.* **2012,** *19* (5), 525-531.
33. Barducci, A.; Bonomi, M.; Parrinello, M., Metadynamics. *Wiley Interdisciplinary Reviews: Computational Molecular Science* **2011,** *1* (5), 826-843.
34. Barducci, A.; Bussi, G.; Parrinello, M., Well-Tempered Metadynamics: A Smoothly Converging and Tunable Free-Energy Method. *Phys. Rev. Lett.* **2008,** *100* (2), 020603.
35. Olsen, J. M. H.; Bolnykh, V.; Meloni, S.; Ippoliti, E.; Bircher, M. P.; Carloni, P.; Rothlisberger, U., MiMiC: A Novel Framework for Multiscale Modeling in Computational Chemistry. *J. Chem. Theory Comput.* **2019,** *15* (6), 3810-3823.
36. Becke, A. D., Density-Functional Thermochemistry. I. The Effect of the Exchange-Only Gradient Correction. *J. Chem. Phys.* **1992,** *96* (3), 2155-2160.
37. Becke, A. D., Density-Functional Thermochemistry. II. The Effect of the Perdew–Wang Generalized-Gradient Correlation Correction. *J. Chem. Phys.* **1992,** *97* (12), 9173-9177.
38. Mackerell Jr, A. D.; Feig, M.; Brooks III, C. L., Extending the Treatment of Backbone Energetics in Protein Force Fields: Limitations of Gas-Phase Quantum Mechanics in Reproducing Protein Conformational Distributions in Molecular Dynamics Simulations. *J. Comput. Chem.* **2004,** *25* (11), 1400-1415.
39. The QM/MM WT-MTD simulations presented here are computed at BLYP level. This functional can understimate the proton transfer barriers (Mangiatordi, G. F.; Brémond, E.; Adamo, C., DFT and Proton Transfer Reactions: A Benchmark Study on Structure and Kinetics. J. Chem. Theory Comput. 2012, 8 (9), 3082-3088). We performed 5 ps unbiased QM/MM simulations using the global hybrid functional B3LYP for both QM/MM WT-MTD involving proton transfer events (MTD.I and MTD.II) (Figure S5 and S7). In both

cases we obtained average structures consistent with the free energy minima in Figure 2B and 2C. Further details are provided in SI. .

40. Elena, A. M.; Meloni, S.; Ciccotti, G., Equilibrium and Rate Constants, and Reaction Mechanism of the HF Dissociation in the HF(H2O)7 Cluster by ab Initio Rare Event Simulations. *J. Phys. Chem. A* **2013,** *117* (49), 13039-13050.

41. Sillanpää, A. J.; Simon, C.; Klein, M. L.; Laasonen, K., Structural and Spectral Properties of Aqueous Hydrogen Fluoride Studied Using ab Initio Molecular Dynamics. *J. Phys. Chem. B* **2002,** *106* (43), 11315-11322.

42. Dereka, B.; Yu, Q.; Lewis, N. H. C.; Carpenter, W. B.; Bowman, J. M.; Tokmakoff, A., Crossover from Hydrogen to Chemical Bonding. *Science* **2021,** *371* (6525), 160.

43. Chon, N. L.; Duster, A. W.; Aydintug, B.; Lin, H., Anion Pathways in CLCF Fluoride/Proton Antiporters. *Chem. Phys. Lett.* **2021,** *762*, 138123.

44. Jülich Supercomputing Centre. (2019). JUWELS: Modular Tier-0/1 Supercomputer at the Jülich Supercomputing Centre. Journal of large-scale research facilities, 5, A135. doi: 10.17815/jlsrf-5-171.

TOC Graphic